We are IntechOpen,
the world's leading publisher of Open Access books
Built by scientists, for scientists

4,000
Open access books available

116,000
International authors and editors

120M
Downloads

154
Countries delivered to

Our authors are among the

TOP 1%
most cited scientists

12.2%
Contributors from top 500 universities

WEB OF SCIENCE™

Selection of our books indexed in the Book Citation Index
in Web of Science™ Core Collection (BKCI)

Interested in publishing with us?
Contact book.department@intechopen.com

Numbers displayed above are based on latest data collected.
For more information visit www.intechopen.com

Chapter

Interface Nerve Tissue-Silicon Nanowire for Regeneration of Injured Nerve and Creation of Bio-Electronic Device

Klimovskaya Alla, Chaikovsky Yuri, Liptuga Anatoliy, Lichodievskiy Volodymyr and Serozhkin Yuriy

Abstract

This overview presents the results of scientific and practical research into the development of the interface "neuron-electronic device" based on silicon nanowire. The work has been carried out for several years by a team of scientists specializing in various fields of science and technology: neuroscience, surface science, nanoelectronics, crystal growth, physics and chemistry of nanotechnology, and nanocomputing. The technology of formation of the interface "nerve fiber-silicon nanowire" was developed. The experiments were performed *in vivo* on Wistar rats. The developed technology was used in the manufacture of implants for the regeneration of the injured sciatic nerve. The results of the studies showed the effectiveness of using such implants not only for the regeneration of nerves with severe injuries but also for the creation of a *bioelectronic* interface for *neurocomputers* that can be used *in vivo* for a long time.

Keywords: interface, silicon nanowires, Wistar rats, sciatic nerve, experiment *in vivo*, laser heterodyne interferometric technique, application of SiNW-FET, physical model of the interface nervous tissue-silicon nanowires

1. Introduction

In the last decade, along with the solution of medical problems on the restoration of the human nervous system by traditional methods, a new direction of neuroscience arose related to the development of hybrid intellect that has to combine the best intellectual resources of human brain and the best achievements of nano- and quantum computing. By the computation speed, modern computers considerably exceed human capabilities, but they have two significant drawbacks. Providing their work with the intellectual capabilities of man using modern nanoelectronics requires considerable power consumption. This leads to an increase in the physical dimensions of the computer in order to provide a thermal regime acceptable for modern nanoelectronics. On the other hand, the human brain, accomplishing a huge amount of work on physical and intellectual interaction and to ensure the correlated work of the organism as a whole, is characterized by *extremely low energy costs* in comparison with quantum computers. Therefore, an idea arisen on creating

a hybrid intellect that physically combines the neural networks of the brain with modern, including quantum, computing devices. The development of such devices required detailed studies of the structure of neural networks of the brain and subsequent modeling of such networks on silicon nanostructures using living neurons or by implanting silicon nanostructures into a neural network of a living organism. The end product of this device will be a hybrid brain that is capable, unlike traditional computers, including quantum ones, to apply both logical and associative methods of solving problems with low energy consumption. The main task of the hybrid brain is to provide a constant two-way communication between the central and peripheral nervous system, which will allow, in extreme case, to constantly monitor the organism as a whole and, if necessary, already in the first stages of the disease, to correct the work of those organs that have deviations from the norm, using, first of all, the internal resources of the body.

By 2015, the strategy for creating hybrid brain has already been developed [1], and a call has been issued [2, 3] to the international community to concentrate scientific and financial resources on the solution of the problem that will make a revolution not only in the field of medicine but also in all spheres of human existence.

Detailed studies of neural networks were started about 10 years ago with the work on the study of the morphology of neural network [4]. Then, a large number of animal studies were made of the relationship between the structure of neural networks and the behavioral characteristics of animals. A detailed review of these studies was published recently [5]. In parallel with studies of the central nervous system and its connection with the peripheral nervous system, work was begun on the creation of a bioelectronic complex on silicon nanostructures with the artificial cultivation of neural networks in a biological environment [6–8]. The results obtained in experiments *in vitro* allowed the transition to animal experiments and then to begin clinical experiments for the treatment of diseases that could not be treated with application of traditional medicine. *Massachusetts General Hospital and Draper Labs* develop a tiny, implanted chip to place it between a patient's skull and scalp. A series of electrodes placed at varying depths in different regions of the brain would record neurological data. In the framework of the program *ElectRx, a closed-loop system* is developed to monitor and to regulate organ functions using the internal resources of the body. *Silent speech information generated directly from the activity of neurons* is involved in speech production via an intracortical microelectrode brain-computer interface [9]. It was shown that *Macaca nemestrina* monkeys can *directly control stimulation of muscles using the activity of neurons in the motor cortex*. Monkeys learned to use artificial connections from cortical cells to muscles to generate bidirectional wrist torques and controlled multiple neuron-muscle pairs simultaneously [10].

Despite encouraging results in the development and testing of bioelectronic complexes capable of recording neural impulses produced by a neuron and transferring them to subsequent processing into a nanocomputer, there are still many unresolved problems, the first of which is the development of a central link of the hybrid intelligence the "neuron-electronic device" interface [11–15]. To date, the greatest difficulty in creating such an interface is the problem of maintaining its working capacity in a living organism for a time comparable to the human lifespan. The most suitable material for creating such an interface is crystalline silicon. First, silicon is a biocompatible material, and, second, it is the main material of nano- and microelectronic technology, which makes it easy to integrate it into electronic circuits for subsequent signal processing. Taking into account the size of neurons (of the order of tens of micrometers), the silicon wires are the most suitable for creating an interface with a neuron. So, in the past decade, the "silicon crystal-nervous tissue" interface has been attracting huge interest. Various designs of electronic circuits of field-effect transistors [16] (SiNW-FET) have been developed. The main attention

in the development of these devices was given to obtaining a high sensitivity of the device for reliable registration of nerve impulses. For this purpose, the SiNW-FET design was developed, in which a dielectric layer between the neuron and the SiNW was created of the ultimate small thickness. The best results on the sensitivity of the SiNW-FET were obtained using the chemical compound poly-L-Lysine as a dielectric between neuron and FET. However, after long-term tests of this design, it was found that the lifetime of such an interface is estimated in a several days or a maximum of a few weeks.

So, a major hurdle in brain-machine interfaces (BMIs) is the lack of an implantable neural interface system that *remains viable for a substantial fraction of the user's lifetime and* the lack of a *high-density, chronic interface to enable recording and stimulation from thousands of sites* in a clinically relevant manner with little or no tissue response remains as one of the grand challenges of the twenty-first century.

The success of the research of our group in experiments on laboratory animals has shown the prospects for application of silicon nanowires in creation of bio-consistent and bioactive implants. The key problem of these works was the study of the biophysical state of the interface "neuron-silicon nanowire" and the development of methods for the purposeful management of its properties. At present, on the basis of this interface, we have developed and patented technology for the manufacture of implants [17], which provides auto-electronic stimulation of the regenerative processes of damaged nerve tissue. The most important feature of the developed technology that significantly distinguishes it from existing ones is to provide conditions for the continuous effective migration of biological cells to the implant site. This feature indicates the promise of its use for the development of neuro-electronic interfaces for neurocomputers, suitable for use over a long period of time, comparable to the years of human life.

In 2-d part of the overview, we present the research on formation of the interface "silicon wire-nerve tissue." Experiments were carried out *in vivo* by simulation of a sciatic nerve injury and following recovery of the injury using silicon nanowires.

In 3-d part, we present experimental techniques used to test how nerve fibers restore functional ability after implantation a conduit with silicon nanowires. In addition to the techniques traditionally used for this purpose, we apply a test to evaluate bidirectional communication between the brain and corresponding peripheral nerve by registration *in real-time in vivo* a nerve displacement initiated due to action potential propagation. We apply additionally SiNW-FET to measure charge state of the interface, when it forms. Furthermore, this experiment gives rise to direct definition of sign and surface charge densities both on silicon wire and nerve fiber in living organism.

In 4-d part we present experimental results on evolution of the restore functionality of the damaged nerve after implantation conduit with silicon nanowires. We analyze prospects to use the interface nervous tissue—silicon nanowire in the global problem brain-computer interface—particularly on possible application quantum HEM device [18] based on silicon nanowires as a nerve pulse binary adder [19, 20].

2. Formation of the interface silicon wire-nerve tissue

The research on formation of the interface "silicon wire-nerve tissue" was carried out *in vivo* on Wistar rats by simulation of a sciatic nerve injury and further replacement fault of the nerve trunk by implant with a set of silicon nanowires.

One of the procedures published in details elsewhere [21, 22] includes several stages: growing of silicon wires, handling the implants, surgical procedure, and various test experiments in vivo for evaluation of motor function recovery by "the method of walking track" [23] and by recording a bilateral interaction between neuronal nets of a brain

and actuators of peripheral nerve by real-time registration nerve displacements due to action potential propagation [24–27] and test experiments in vitro to examine morphological features of the interface by optical and electron transmission microscopy.

2.1 Growth of silicon wires

Silicon wires (see **Figure 1**) were grown by the technology developed by Sandulova et al. [28]. This technology is based on a method of gas-phase reaction in a sealed tube at a temperature gradient. In order to provide the chemical reactions and to stimulate rapid growth of the wires, we used bromine and gold.

For growing wires with a prespecified type and value of conductivity, we added doping impurities into hot part of the tube. Due to differences in the reaction-binding energies of gold and the doping impurities with bromine, the temperature gradient provides a different amount of precipitation of these materials along the tube. That is why grown silicon wires are distributed along the tube by size (diameter, length) and by the level of doping [29, 30]. The thinner the diameter of a wire is, the smaller is the concentration of dopants. The diameter of the grown wires ranges from 10 nm to several tens of microns. Their length varies in a range from tens of microns up to a few centimeters. Furthermore, the shape of wires depends on their diameter, too.

The wires, which diameter was of nanometers, were cylindrical, while the wires with much greater diameters were hexahedral.

2.2 Handling the implants

Wires for preparation of implants are shown in **Figure 1**. Making of implant started from dividing the wires by diameters. The prepared set of nanowires was treated for purification of a surface in different etchants. Thereupon, the wires were oxidized by storage under ambient atmosphere at room temperature. The thickness of silicon oxide does not exceed one to two nanometers. Just before surgical operation, an antispiking gel ("Mesogel," Linteks Ltd., Russian Federation) was introduced into the aorta extracted from another rat. In order to avoid a rejection of
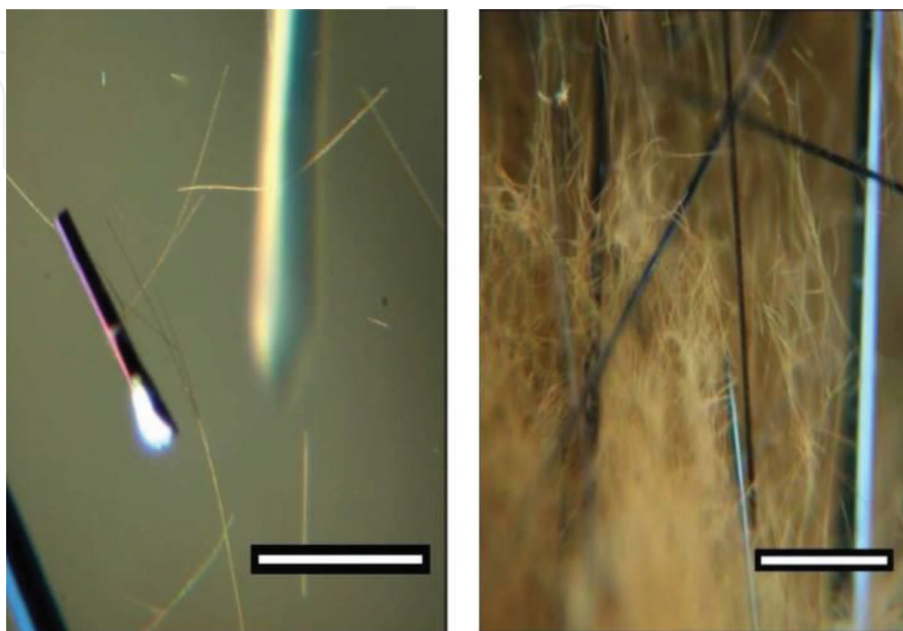

Figure 1.
Wires for preparation of implants. Scale bar is 80 μm on the left and 250 μm on the right side of the figure.
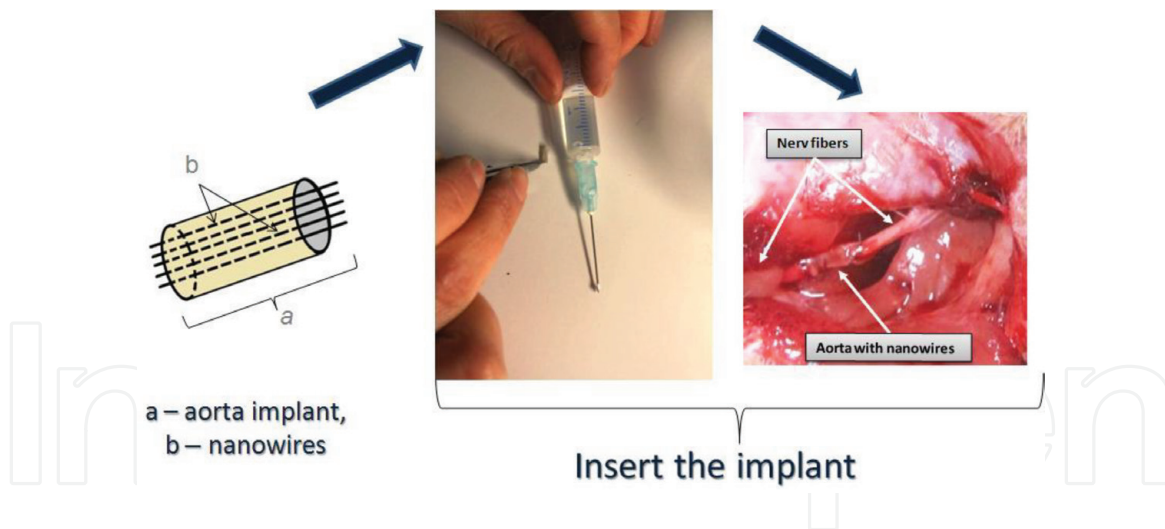
Figure 2.
Surgical procedure.

the transplant, the aorta has been prefrozen in liquid nitrogen. Then, the set of the wires was placed into the gel and oriented along an axis of the aorta.

2.3 Surgical procedure

Experiment was carried out on rats, weighing 180–250 g, that were housed in standard conditions with free access to food and water and natural light-dark cycle. The rats were randomly divided into several groups. Under thiopentone general anesthesia (40–60 mg/kg intraperitoneally), right sciatic nerve of animals were exposed in middle third, separated from surrounding tissues for approximately 10 mm in length, and isolated from underlying muscles. For the animals of one group, after dissection of sciatic nerve, we inserted the implant (**Figure 2**). Animals of the other groups were used for trauma simulating of the nerve and as sham-operated ones.

Animal care, housing, and all experiments were performed in accordance with the National Institutes of Health guide for the care and use of laboratory animals (NIH Publications No. 8023, revised 1978). The research was approved by Bioethical Committee for human subjects or animal research at Bogomolets National Medical University, December 30, 2015.

3 Methods for evaluation of nerve recovery after implantation

Along with traditional methods of evaluation of a nerve recovery, we first used laser heterodyne interferometric techniques that give rise to record *in vivo* in real time an evolution of bilateral interaction of a brain and peripheral nerve [31] that reflect a quality of the nerve recovery.

3.1 Experiment *in vivo* for evaluation of motor function recovery

In the course up to 5 months, rats were tested on a degree of nerve regeneration. For evaluation of motor function recovery, we used "the method of walking tracks" [23]. The degree of motor function recovery was determined by the shape and size of prints of hind paws of animals when they pass through a narrow corridor. For quantitative assessment of sciatic function index (SFI), we used print length, toe spread, and intermediate toe spread on the prints of both post-operated and healthy hind limbs.

3.2 Experiment *in vivo* for evaluation of a bilateral interaction of a brain and peripheral nerve

To evaluate a recovery of bilateral interactions between neuronal net of a brain and actuators of peripheral nerve, we designed a setup on detection of nanometer displacement of nerve fibers [24–27] using laser heterodyne interferometric techniques with next specifications:

- Laser wavelength 0.63 μm

- Power of the probing radiation 1 mW

- Bandwidth of the receiver 1–30 KHz

- Noise level at frequency 1 KHz with bandwidth 3 KHz on distance 1 m about 0.1 nm

- Optical setup for detecting the surface displacement that is accompanying neuronal activity is presented in **Figure 3**.

The installation includes a laser heterodyne displacement meter, a computer for controlling the meter, and a computer for processing and displaying measurement results. The principle of operation of the displacement meter is based on detecting changes in the phase of scattered radiation from the object under study, relative to the phase of radiation of the laser heterodyne. The information signal is a phase-modulated variable component of the photodetector current, which is formed as a result of interference of laser radiation and scattered radiation from the object under study, in the current case from the nerve of rat.
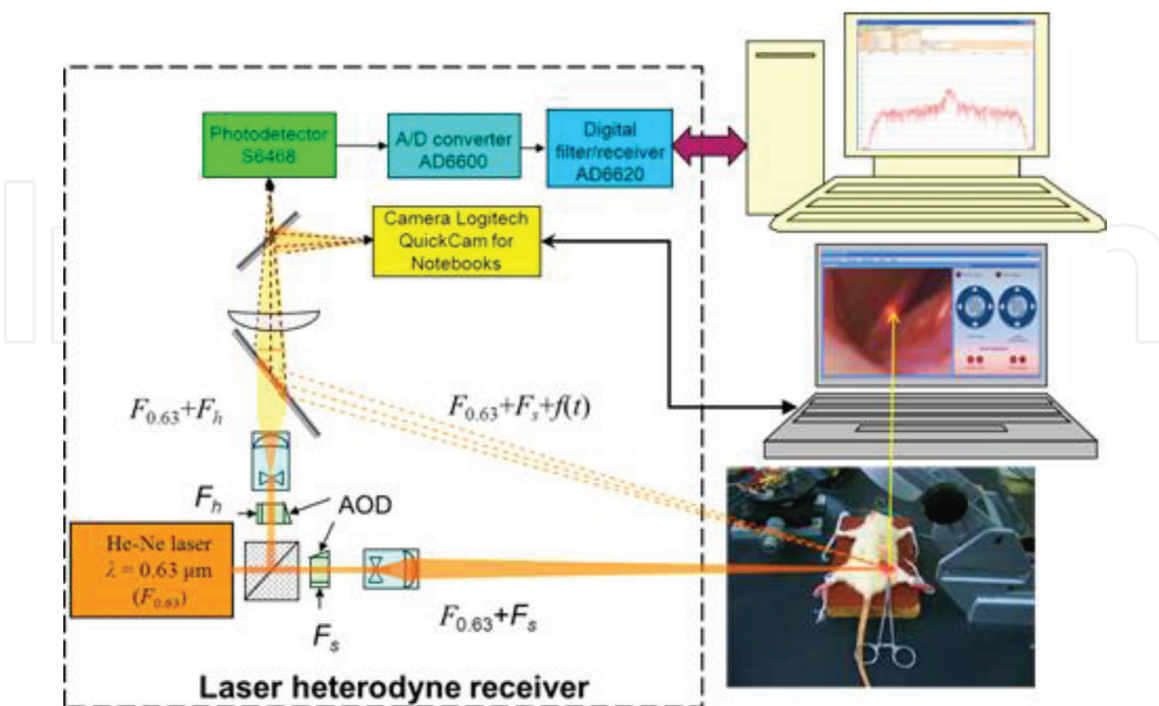

Figure 3.
Optical setup for detecting neuronal activity.

3.3 Examination of morphology of the interface

Around 6 weeks after the implantation, animals of the first group were taken out of the experiment by decapitation with the use of an overdose of thiopental anesthesia. Nerves with the implant were extracted, and slices were produced using a cryotome (MK-25, "Tekhnolog" Russia). Thereupon, the slices were stored during the day in 10% neutral formalin, next rinsed in distilled water, and fixed on a microscope slide. For the purposes of microscope investigation of the nerve fibers, samples were stained with silver nitrate [32]. Prepared slices of the interface "nerve fiber-silicon wire" were examined by light microscopes Carl Zeiss NU-2E and Olympus BX 51 equipped with a digital camera and transmission electron micro-scope TEM-125K (SELMI, Ukraine).

For light microscopy, material was prefixed by intracardiac perfusion with 10% formalin in 0.1 M phosphate buffer, postfixed in 10% formalin, dehydrated, and embedded in paraffin. Sections were cut and strained with hematoxylin-eosin, by the van Gieson method, impregnated with nitric silver. For TEM, material was prefixed by intracardiac perfusion with 1% glutaraldehyde in 0.1 M phosphate buffer, postfixed in 1% glutaraldehyde, 1% osmium oxide, dehydrated, and embedded in epone-araldite. Semi-thin and ultrathin sections were cut, contrasted by lead citrate and acetate.

3.4 Experiment on ascertain energy state of the interface nerve tissue-silicon nanowire

To elucidate the energy state of both constituents of the interface, we carry out experiment with application of SiNW-FET biosensor based on SOI structure with two gates [33–35] as the sensor element to evaluate charge states of the surface of silicon nanowire and the nerve fiber during the interface formation. A schematic representation of this transistor is shown in **Figure 4**.

In this transistor, the substrate is used as a control gate (back-gate, BG), modulating their conductivity. An analyte, which adheres to the free surface of the transistor, plays the role of the second gate (virtual local gate). If the charge at the surface of the nanotransistor changes due to adsorption of the analyte, so will change the conductivity of the nanotransistor and will shift its current-voltage $I_{ds}(V_{bg})$ characteristic along voltage axis. A sign and value of the shifting allow determining both the sign and the density of the adsorbed charge.
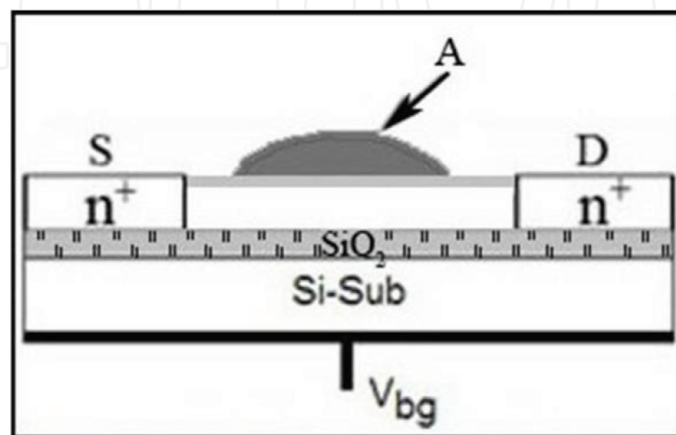

Figure 4.
Schematic presentation a dual-gated SiNW-FET biosensor based on SOI structure.

To elucidate how the charge state of the nanotransistor surface changes during the interface formation, we carried out experiment *in vitro* and studied the current-voltage characteristics $I_{ds}(V_{bg})$ in three cases: (1) initial state of the surface of the nanotransistor (without any analyte, i.e., a free surface covered with native oxide only), (2) the surface of the nanotransistor in contact with the physiological environment, and (3) the surface of the nanotransistor after adherence of a neuron when it is immersed into the physiological environment. The measured current-voltage characteristics for these three cases give rise to calculate the surface density of the initial charge on silicon nanowire (biosensor), after adherence of components of the physiological environment and after adherence of a neuron as well.

4. Results and discussion

4.1 Evaluation of motor function

Results on recovery motor function of the limb by "the method of walking tracks" [23] are presented in **Figure 5**. It is seen that the sciatic function index (SFI) related to motor function of the limb, being normal before simulation of a sciatic nerve injury, instantly after implantation sharply decreases to abnormal state. However, in postoperative period about several months, functionality of the limb, even if slowly, improves.

4.2 Evaluation of bidirectional communication between the brain and peripheral nerve

To evaluate regeneration of sciatic nerve *in vivo*, we used additionally the laser heterodyne interferometric technique that allows in real-time record of efferent and afferent nerve impulses that provide bidirectional communication between neuronal net of a brain and actuators of peripheral nerve, notably a limb.

Propagation of nerve electrical impulses along the axon is known, to be accompanying several other phenomena such as displacements of the axon, propagation of elastic and thermal waves, and magnetic oscillations as well [36, 37].
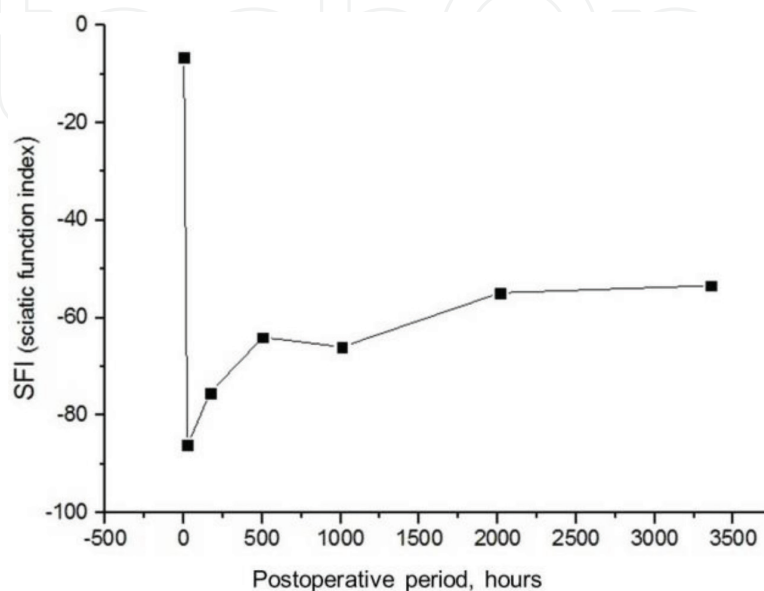

Figure 5.
Evolution of the motor function recovery in postoperative period.

In this work we study in real-time *in vivo* displacements of the nerve induced by nerve electrical impulses propagation. First of all, it should be noted that we measure the sum of the displacements of a bundle of the axons that forms the sciatic nerve. That is why the recorded displacements present the sum of independent cycles of a large number (about 1000 [38]) of the axon excitations. Consequently, we cannot observe a single excitation of regularly shaped spikelike to the observed *in vitro* on squid giant axon [39]. Furthermore, a magnitude of the spikes observed in the current experiment considerably exceeds the observed on a single axon.

The first step of our measurement was recording *in vivo* in real time the displacements of healthy nerve that is shown in **Figure 6** (top line). The next step is dissection of the healthy nerve and a measurement of activity in both dissected proximal and distal parts of the nerve presented in **Figure 6** (center and bottom lines). From a comparison of the intensities of the nerve impulse generation of a healthy nerve, **Figure 6** (top line), and the proximal and distal parts of the dissected nerve (central and bottom line accordingly), it is seen that intensity of nerve impulses propagation persists enough high, especially on the proximal part.

The second step is to carry out surgical operation on implantation of the aorta filled by the silicon nanowires. Then, we measure nerve displacements immediately after implantation (**Figure 7**) in three places of the post-operated nerve: proximal part, implant and distal part.

It is seen that immediately after implantation (**Figure 7**), the intensity of the nerve impulses generation on the proximal segment of the nerve slightly decreased,
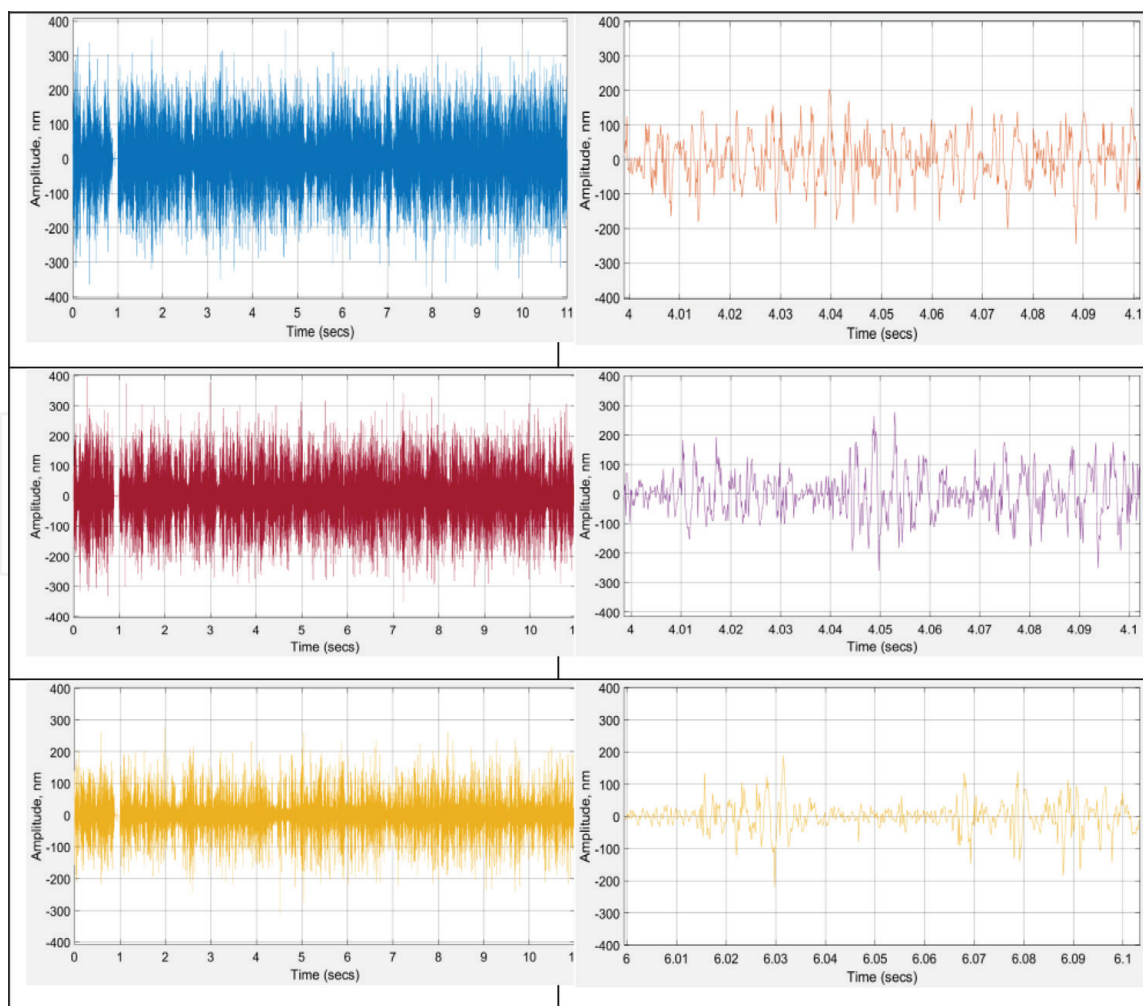

Figure 6.
Record in real-time in vivo displacements of the healthy nerve (the top line) and after dissection of the nerve (the center line, the proximal part; the bottom line, the distal part of the nerve).
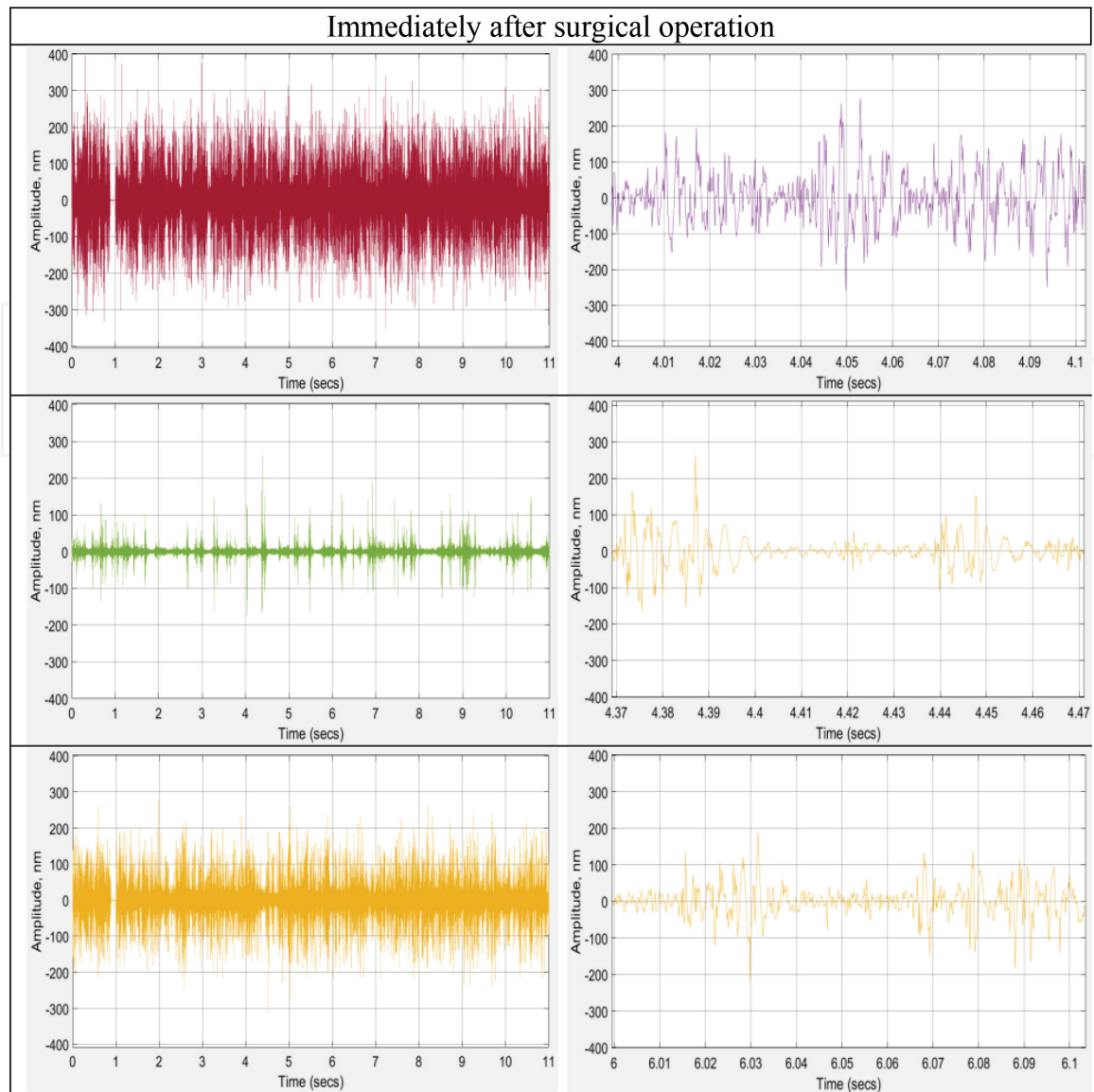
Figure 7.
Record in real-time in vivo displacements of the nerve immediately after implantation in three places of the post-operated nerve: the proximal part (the top line), the implant (the central line) and the distal part (the bottom line).

which could be expected, because this part of the nerve no longer receives signals generated in the paw. Generation of impulses produced in the paw (distal portion of the nerve) decreased more significantly. Nerve impulses in the area of the implant immediately after surgery are practically absent (**Figure 7**).

However, after 3 months the passage of nerve impulses through the regenerated nerve is already restored (**Figure 8**). Intensity propagations of nerve impulses through implant and distal parts are similar.

We conducted up to 20 experiments to study the passage of nerve impulses through the regenerating nerve. Summarizing results of all the test experiments, we can conclude that quality of restoration of the limb functionality depends on duration of postoperative period, number of silicon wires filling a gap, and physical properties of the wires.

4.3. Morphology of the interfaces nerve fiber-silicon nanowires

To understand the mechanism of neural tissue regeneration, a series of experiments were carried out to elucidate the morphological features of the interface "neuron-silicon nanowire." This research was published elsewhere [21, 22, 40],
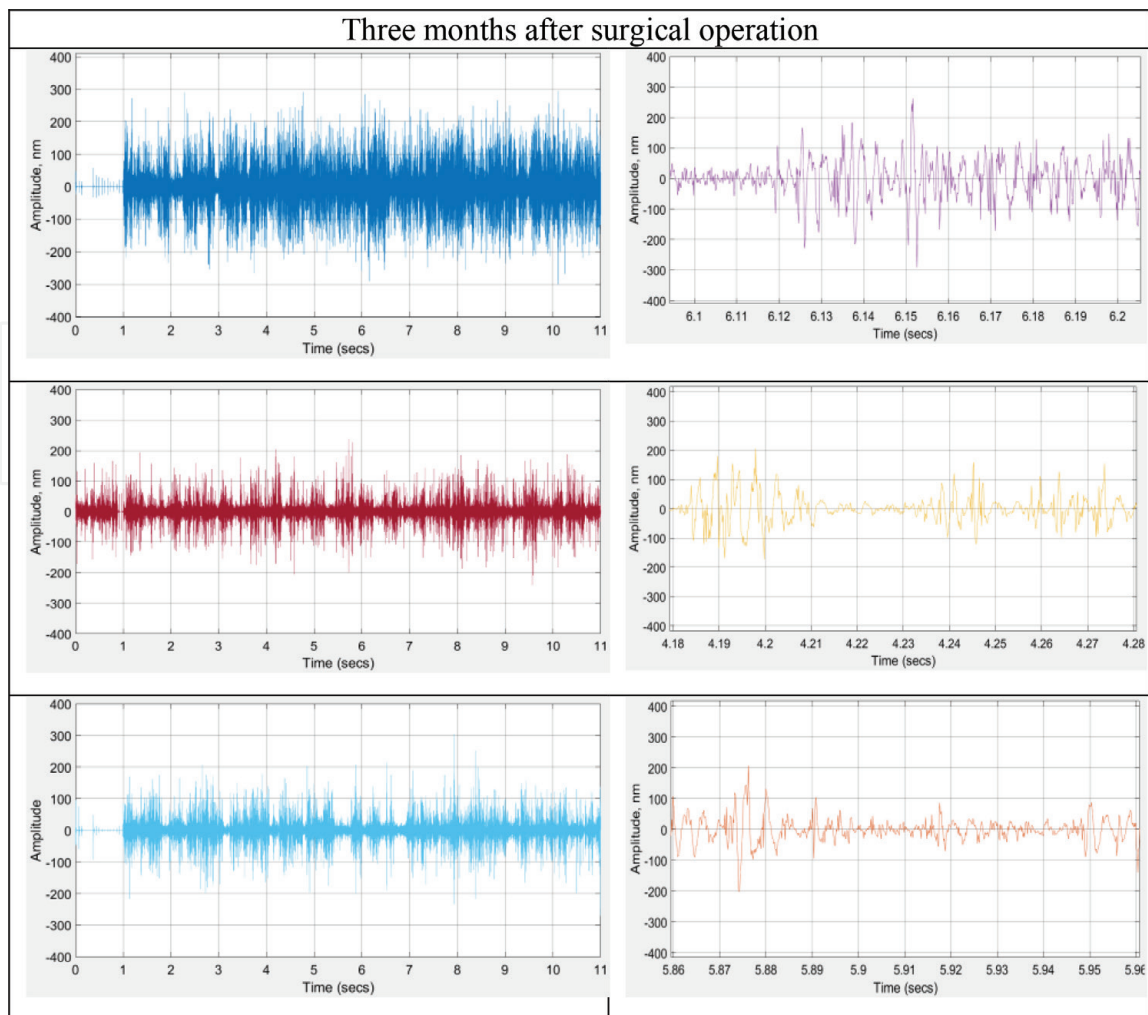
Figure 8.
Record in real-time in vivo displacements of the nerve after 3 months post-implantation in three places of the post-operated nerve: the proximal part (the top line), the implant (the central line), and the distal part (the bottom line) of the nerve.

while the main results and discussion are given below. The interfaces prepared *in vivo* were examined in various post-operation periods ranging from 3 weeks up to 12 months. The growing nerve fibers formed within the short period were unmyelinated, while the others had myelin sheath whose thickness depended on the length of the postoperative period. Micrographs of the interfaces "nerve fiber-silicon wire" studied in light microscope are presented in **Figures 9** and **10a**.

Before analyzing the micrographs, it is worthy to point out a specification of the preparation of slices that induced high difference in mechanical strength of nerve fiber and silicon wire. We attempted to prepare all the slices oriented primarily along the large axis of the wires. High deviation from this direction resulted in breaking off and falling out a piece of the crystal and in a persistence of a mark of the crystal-removed part as a residual of the biomaterial.

This may be seen in the micrographs of **Figure 9(a, b)**. Slight deviation from this direction resulted in persistence of beveled cut of biomaterial placed on the crystal surface. In case, if the persistent layer of biomaterial is sufficiently thin, then one can see crystals, which accrete from every side by arrays of regenerating nerve fibers. In another case, interface "nerve fiber-silicon wire" is clearly seen along all lengths of the wire (see **Figure 9c**). High sensitivity of the nerve fibers to silicon wires is clearly seen from **Figure 9d**, which presents how the array of growing nerve fibers changes a direction of their growth, when it meets the silicon wire, adsorbs on a surface of the wire, and carries on further growth across the surface.
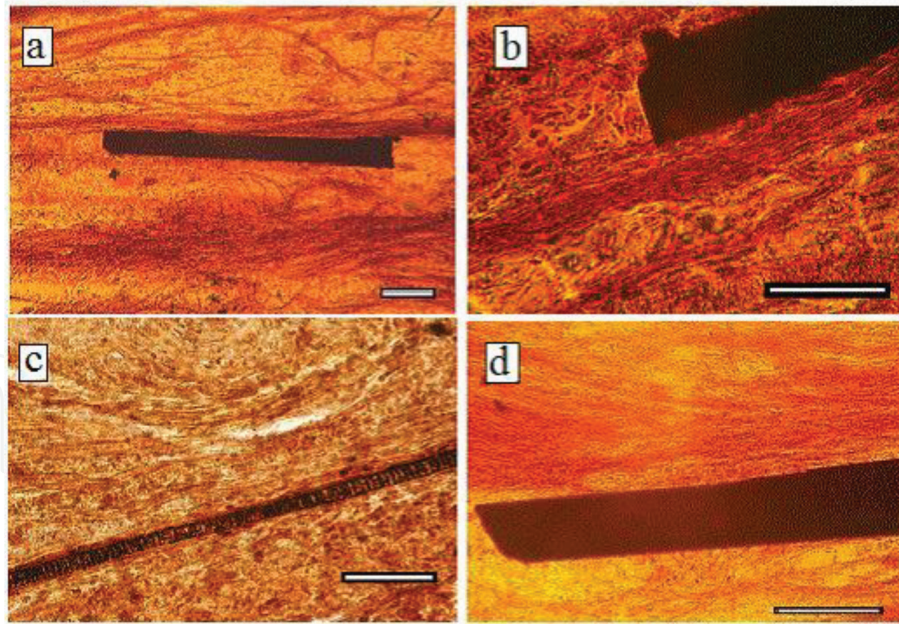
Figure 9.
Micrographs of the affected nerve with the implanted silicon wires. Scale bar is: (a) 150 μm, (b) 50 μm, (c) 60 μm, and (d) 80 μm.
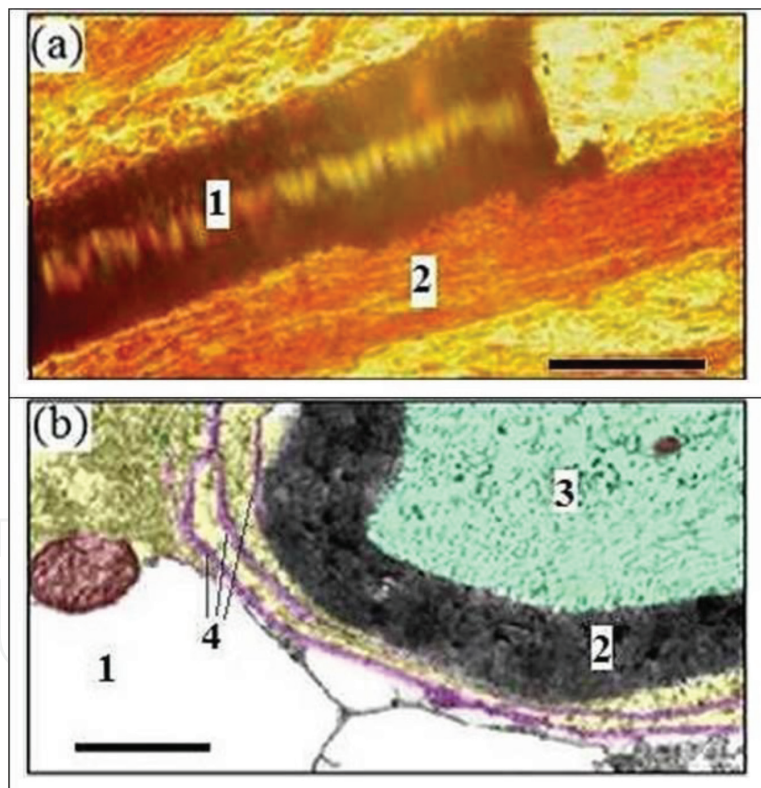

Figure 10.
Micrographs of the interfaces: (a) made with light microscope, the slice is impregnated with nitric silver; plane of the slice coincides with the long axis of the silicon wire; here 1 is the silicon wire, and 2 is a bundle of the newly formed nerve fibers; (b) made with transmission electron microscope, the slice treated with 1% water solution of osmic acid; plane of the slice was perpendicular to the long axis of the silicon wire; here 1 is the silicon wire, 2 is myelin sheath, 3 is axoplasm, and 4 is new layers of the myelin sheath formed of Schwann cells. Scale bar: (a) 40 μm and (b) 50 nm.

In all these cases, though their variety, we can conclude on high sensitivity of the growing nerve to the surface of silicon crystals. Typical micrographs of the "silicon wire-nerve fiber" interfaces made with the light and transmission electron microscopes are shown in **Figure 10**.

Examination of the interface with different magnifications allowed seeing general picture of the growing nerve fibers in the vicinity of the silicon wire and a set of various cells supporting growth of the nerve. In **Figure 10** a micrograph of the interface made with light microscope demonstrates how a bundle of the newly grown young nerve fibers tightly adhere to the silicon wire. The micrograph of the interface made with transmission electron microscope (**Figure 10b**) shows how the newly formed layers of cell membrane of regenerating nerve fiber adhere to silicon crystal. The distance between membrane and silicon wire is less than a few nanometers. Having analyzed a great number of micrographs, we can conclude that young regenerating nerve fibers adhere to the surface of silicon crystals.

To understand the affinity of the nerve fiber to the surface of the silicon nanowires found experimentally, we have to consider the composition and the energy state of both constituents of the interface, i.e., the nerve fiber and the silicon wire.

The energy state of the near-surface region of the silicon wire at room atmosphere is shown in **Figure 11a**. In our experiment, we used silicon wires doped by boron that means that position of the Fermi level in the bulk of the crystal E_f is placed nearby the top of the valence band E_v.

A specific lattice restructuring of a few external atomic layers proper to the silicon surface is known [41] to initiate two energy bands located immediately at the surface. Density of the states in each of these bands is very high and approaches density of atoms at the surface ($\sim 10^{14}$ cm^{-2}); therefore, the Fermi level at the surface is placed near the middle of the energy gap E_i, and its position slightly depends on doping [42, 43] and growth of a thin native oxide as well. However, in p-type of silicon, which is used in our experiment, a positive charge at the surficial bands exceeds the negative one.
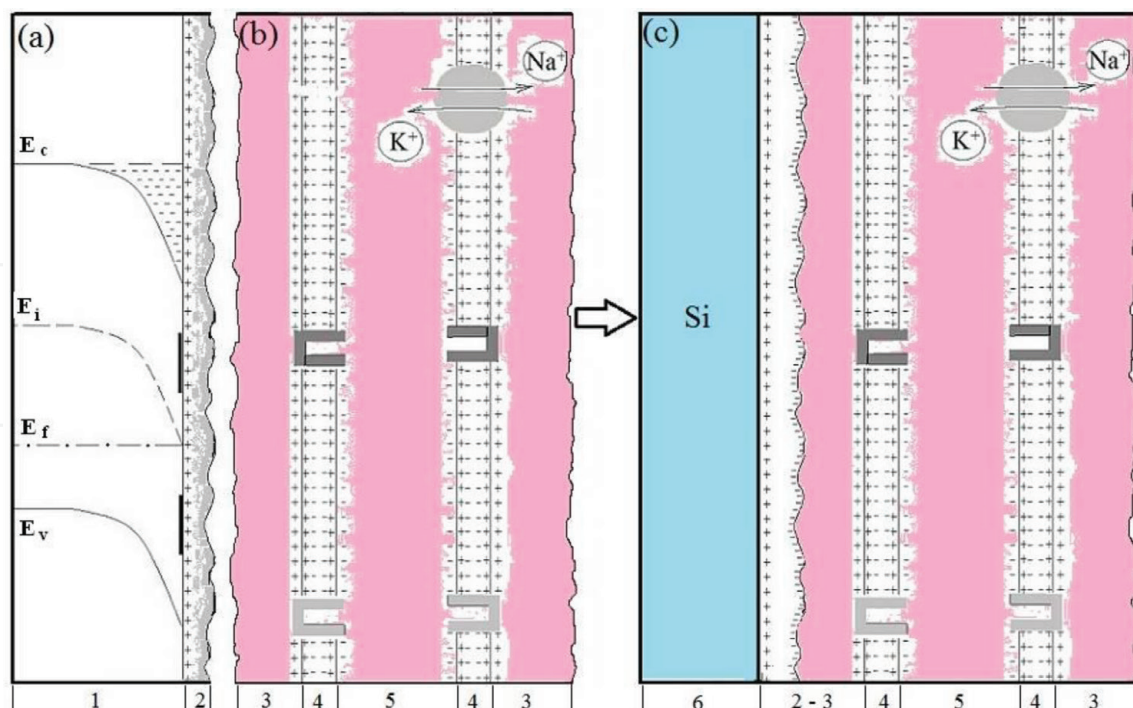

Figure 11.
(a) The near-surface region of silicon wire, where 1 is the energy structure of the near-surface region of the silicon wire and 2 is a native oxide layer on the nanowire surface. (b) A structure of the membrane of nerve fiber (axon) in the living organism, where 3 is the extracellular physiological environment, 4 is the axon membrane composed of phospholipids molecules, and 5 is the axoplasm. (c) A morphology of the "silicon wire-nervous tissue" interface generated in the living organism, where 6 is the silicon wire, 2–3 are the interface of a negatively charged native oxide and positively charged outer surface of the nerve fiber membrane, 4 is the axon membrane, and 5 is the axoplasm.

Thus, the silicon wire being at vacuum or covered by the thin native oxide is entirely neutral, though the external surface of the silicon wire is charged positively.

The structure of the nerve fiber membrane inside a living organism is shown in **Figure 11b**. In our case preparation of the interface from the sciatic nerve of rats, the axon membrane is composed of phospholipid molecules that are known [44] to consist of polar heads and nonpolar tails and form the membrane in a shape of bilayer. It is worthwhile to emphasize that the outer side of the polar heads is charged positively. Surface density of this charge, according to the Richardson structure model, equals about 2×10^{13} cm^{-2}. So, a large positive charge of about 2×10^{13} cm^{-2} is permanently located at the outer side of the membrane.

Summarizing the above consideration, we can draw the following conclusion. If the near-surface region of the silicon nanowire conserves its charge state inside the living organism, then the silicon wire and the nerve fiber are similarly charged and have to repulse each other. Nevertheless, we do observe a strong adherence of the nerve fiber to the silicon nanowire that allows supposing that the physiological environment (interstitial fluid, cell cytoplasm, etc.) contributes to the formation of the interface. Analyzing how the environment may influence the charge state of silicon nanowire, we paid attention to the main properties of the physiological environment. About 80% of the environment consists of water and its pH > 7. On the other hand, thin native oxide layer, that covers the wires, is known [45] to consist primarily of intermediate oxidation states of Si atoms, in particular, $Si^{1+}(Si_2O)$, $Si^{2+}(SiO)$, and $Si^{3+}(Si_2O_3)$. Thus, we can suppose that sub-oxidized Si atoms chemically react with OH$^-$ radicals of the environment, charge the surface of the nanowire negatively, and, thereby, provide Coulomb attraction between silicon wire and nerve fiber. To validate this assumption, we used a model experiment on contact of the nerve cells with silicon nanowire in the electrolyte with pH > 7, close to the physiological environment.

4.4 Evaluation of the charge state of the interface nerve tissue-silicon nanowire

In this experiment SiNW-FET based on SOI structure with two gates [32–34] has been used as the sensor element to evaluate charge states of the silicon nanowire during the interface formation.

An optical image of the nerve cell after its adherence on SiNW-FET is shown in **Figure 12**. In this transistor, the substrate is used as a control gate (back-gate, BG), modulating their conductivity. An analyte which adheres to the free surface of the transistor plays the role of the second gate (virtual local gate). If the charge at the surface of the nanotransistor changes due to adsorption of the analyte, so
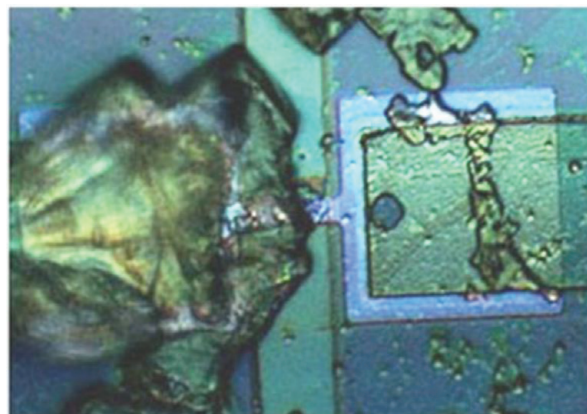

Figure 12.
Micrograph of a neuron adhering to the surface of biosensor.

will change the conductivity of the nanotransistor and will shift its current-voltage $I_{ds}(V_{bg})$ characteristic along voltage axis. A sign and value of the shifting allow determining both the sign and the density of the adsorbed charge.

To elucidate how the charge state of the nanotransistor surface changes in contact with the physiological environment and after adherence of a neuron, we studied current-voltage characteristics $I_{ds}(V_{bg})$ in three cases: (1) initial state of the surface of the nanotransistor (without any analyte, i.e., a free surface covered with native oxide only), (2) the surface of the nanotransistor in contact with the physiological environment, and (3) the surface of the nanotransistor after adherence of a neuron when it is immersed into the physiological environment. The current-voltage characteristics for these three cases are shown in **Figure 13**.

It is seen that, when we immerse the nanotransistor into the physiological environment, the current-voltage characteristics shift to the greater voltage V_{bg} that corresponds, by conditions of our experiment, to a negative charging of the surface of the nanotransistor. Then, we immerse a neuron into the physiological environment and observe its adherence to the surface of the nanotransistor (**Figure 12**). The adherence of the neuron is accompanied by shifting of the current-voltage characteristic in the opposite direction, in particular, to the smaller voltage V_{bg} that means an accumulation of a positive charge at the surface of the nanotransistor. Knowledge of the shifting of the current-voltage characteristics and geometric parameters of the nanotransistor allows calculating the surficial charge at the surface of the nanotransistor induced by the adherence of the analyte. We calculated the surface density of this charge after adherence of components of the physiological environment and after adherence of a neuron as well. We found that the charge accumulated in physiological environment on the surface of the silicon nanotransistor is negative and its density equals $\sim 1 \bullet 10^{14}$ cm^{-2}. On the other hand, the adsorption of a neuron initiates accumulation of a positive charge on the surface of nanotransistor. The density of this charge is equal to $\sim 2 \cdot 10^{13}$ cm^{-2}.

So, the experiment *in vitro* proved the above-made assumption about chemical reaction of native oxide with OH$^-$ radicals and, hereby, negatively charging a
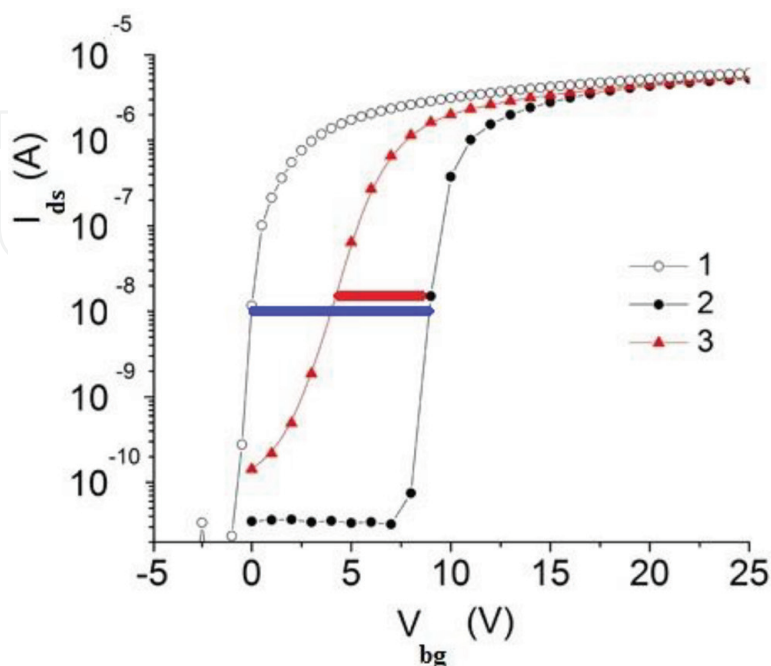

Figure 13.
Current-voltage characteristics $I_{ds}(V_{bg})$ for three cases of the surface of biosensor. (1) The surface covered by native oxide (without any analyte), (2) the surface in contact with the physiological environment, and (3) the surface in contact with adsorbed neuron that was immersed into the physiological environment.

surface of the native oxide of silicon wire. Furthermore, the density of the positive charge accumulated at the silicon nanotransistor after adsorption of the neuron coincides with the known value of the surface density of polar head of phospholipid molecules by the Richardson structure model [44]. So, from the *in vitro* experiment, we can draw a conclusion on the Coulomb origin of the interface formation and present morphology of the "silicon wire-nervous tissue" interface as it is shown in **Figure 11c**.

It is also evident that a propagation of the nerve impulse through the nerve fiber has to occur in a quite different way than the case when the nerve impulse passes through a free nerve fiber. A charge state of the formed interface during propagation of nerve impulse schematically is shown in **Figure 14**.

At a normal (resting) state of the nerve fiber, besides a permanent positive charge at the outer side of the membrane, there is an additional positive charge located inside the extracellular medium and the negative charge located inside the axoplasm. These charges produce potential difference across the axon membrane, the so called resting potential (V_{rest} ~ 70 mV) that acts throughout the entire length of the nerve fiber in a normal (resting) state of the nerve. However, when a nerve impulse passes along the nerve fiber, it reverses the potential difference across the axon membrane, the so called, "action potential" (V_{action} ~ 40 mV). So, propagation
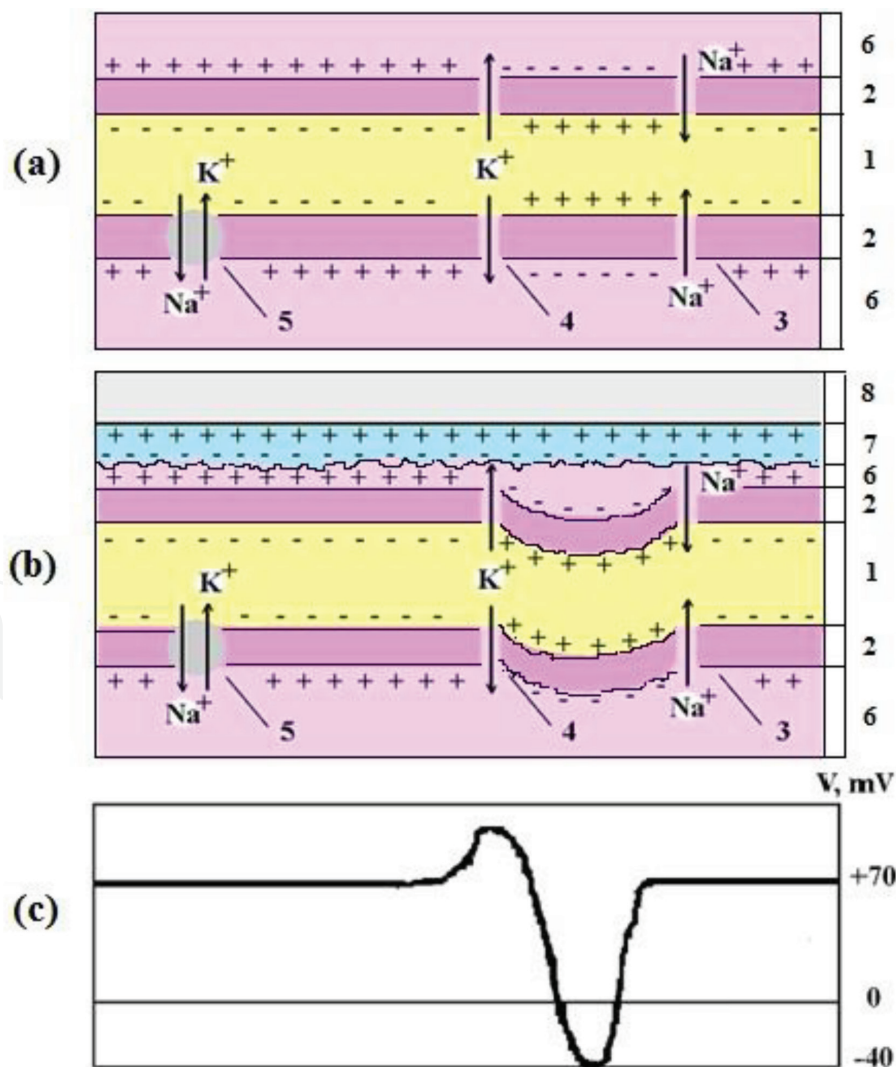

Figure 14.
Charge state of the nervous fiber in physiological environment (a) and charge state of the interface (b) during a nerve impulse propagation (c). Here 1 is the axoplasm; 2 is the axon membrane; 3, 4, and 5 are the ion channels; 6 is the extracellular physiological environment; 7 is the native oxide with negative charge on its surface; and 8 is the silicon wire.

of the nerve impulse along the nerve fiber has to be accompanied by a flexural wave in the nerve due to recharge of the external side of the membrane and subsequent changing of the Coulomb attraction of the nerve fiber to the silicon wire by the Coulomb repulsion. Additionally, propagation of the nerve impulse has to generate an electronic surficial wave in a space charge region of the silicon wire. The latter may be used for extracellular recording of neuronal signal. Details of this process have to depend strongly on properties of silicon wires and call for further research.

5. Conclusion

Here we presented the study of the "silicon wire-nerve tissue" interface formed both *in vivo* and *in vitro* experiments. We have shown experimentally that there is a very good adhesion, of a nerve tissue to silicon wire, covered by thin native oxide, in the living organism. We analyzed the morphology of the interface from a physical point of view taking into account the energy structure of silicon surface, morphology of the surface layer of nerve fiber, and the composition of nutrient medium as well. Result of the analysis is indicated on Coulomb interaction between the constituents of the interface. To verify this conclusion, we carried out experiment using doubly gated SOI-SiNW-FET that is given rise to measure the surface densities of the charge both on the surface of silicon wire and on the surface of nerve fiber. This experiment has shown that strong adhesion of silicon wire and nerve fiber is given rise to Coulomb mutual attraction of the oppositely charged surfaces of the nerve fiber and silicon wire. We analyzed Coulomb interactions at the interface during propagation of a nerve impulse and concluded that nerve impulse has to initiate a flexural wave in the nerve fiber and to generate an electronic surficial wave in a space charge region of silicon wire. Moreover, the flexural wave has to provide *metabolism in the nerve fiber and, hereby vital capacity of the interface*. On the other hand, the electronic wave in the space-charge region of silicon nanowire allows using it for extracellular recording of neuronal signal. So, it is evident that the proposed method of the interface "nervous tissue-silicon nanowire" preparation is promising for application in the global project brain-computer interface, particularly on possible application quantum HEM device based on silicon nanowires as a nerve pulse binary adder.

Conflict of interest

We have no conflicts of interest to disclose.

Author details

Klimovskaya Alla[1]*, Chaikovsky Yuri[2], Liptuga Anatoliy[1], Lichodievskiy Volodymyr[2] and Serozhkin Yuriy[1]

1 V.E. Lashkaryov Institute of Semiconductor Physics, Kyiv, Ukraine

2 O.O. Bogomolets National Medical University, Kyiv, Ukraine

*Address all correspondence to: kaignn@gmail.com

IntechOpen

References

[1] Chang Edward F. Towards large-scale, human-based, mesoscopic neurotechnologies. Neuron. 2015;**86**(1):68-78. DOI: 10.1016/j.neuron.2015.03.037

[2] Brose K. Global neuroscience. Neuron. 2016;**92**:557-658

[3] Fairhall A, Svoboda K, Nobre AC, Gradinaru V, Nusser Z, Ghosh A, et al. Global collaboration, learning from other fields. Neuron. 2016;**92**:561-563. DOI: 10.1016/j.neuron.2016.10.040

[4] Luo L, Callaway EM, Svoboda K. Genetic dissection of neural circuits. Neuron. 2008;**57**:634-660. DOI: 10.1016/j.neuron.2008.01.002

[5] Luo L, Callaway EM, Svoboda K. Genetic dissection of neural circuits: A decade of progress. Neuron. 2018;**98**(2):256-281. DOI: 10.1016/j.neuron.2018.03.040

[6] Lee K-Y, Shim S, Kim I-S, Oh H, Kim S, Ahn J-P, et al. Coupling of semiconductor nanowires with neurons and their interfacial structure. Nanoscale Research Letters. 2010;**5**:410-415. DOI: 10.1007/s11671-009-9498-0

[7] Kwiat M, Elnathan R, Pevzner A, Peretz A, Barak B, Peretz H, et al. Highly ordered large-scale neuronal networks of individual cells – Toward single cell to 3D nanowire intracellular interfaces. ACS Applied Materials & Interfaces. 2012;**4**(7):3542-3549. DOI: 10.1021/am300602e

[8] Lee K-Y, Kim I, Kim S-E, Jeong D-W, Kim J-J, Rhim H, et al. Vertical nanowire probes for intracellular signaling of living cells. Nanoscale Research Letters. 2014;**9**(1):56-63. DOI: 10.1186/1556-276X-9-56

[9] Brumberg JS, Nieto-Castanon A, Kennedy PR, Guenther FH. Brain–computer interfaces for speech communication. Speech Communication. 2010;**52**(4):367-379. DOI: 10.1016/j.specom.2010.01.001

[10] Moritz CT, Perlmutter SI, Fetz EE. Direct control of paralyzed muscles by cortical neurons. Nature. 2008;**456**(7222):639-642. DOI: 10.1038/nature07418

[11] Coffer JL, editor. Semiconducting Silicon Nanowires for Biomedical Applications. Cambridge: Woodhead Publishing Series in Biomaterials; 2014. 296 p. ISBN: 9780857097712 (online)

[12] Wark HA, Sharma R, Mathews KS, Fernandez E, Yoo J, Christensen B, et al. A new high-density (25 electrodes/mm^2) penetrating microelectrode array for recording and stimulating sub-millimeter neuroanatomical structures. Journal of Neural Engineering. 2013;**10**(4):045003. DOI: 10.1088/1741-2560/10/4/045003

[13] Kruskal PB, Jiang Z, Gao T, Lieber CM. Beyond the patch clamp: Nanotechnologies for intracellular recording. Neuron. 2015;**86**(1):21-24. DOI: 10.1016/j.neuron.2015.01.004

[14] Winslow BD, Christensen MB, Yang WK, Solzbacher F, Tresco PA. A comparison of the tissue response to chronically implanted Parylene-C-coated and uncoated planar silicon microelectrode arrays in rat cortex. Biomaterials. 2010;**31**(35):9163-9172. DOI: 10.1016/j.biomaterials.2010.05.050

[15] Kim Y, Romero-Ortega MI. Material considerations for peripheral nerve interfacing. MRS Bulletin. 2012;**37**(6):573-580. DOI: 10.1557/mrs.2012.99

[16] Noy A. Bionanoelectronics. Advanced Materials. 2011;**23**(7):807-820. DOI: 10.1002/adma.201003751

[17] Chaikovsky Yu B, Klimovskaya AI, Vysotskaya NA, Korsak AV, Likhodiievskyi VV. Method of Electrostimulation of Regeneration of Nerve Tissues using Silicon Nanowires. Patent UA No. 104557. Bull. No. 3; 2016

[18] Klimovskaya AI, Raichev OE, Dadykin AA, Litvin Yu M, Lytvyn PM, Prokopenko IV, et al. Quantized field-electron emission at 300K in self-assembled arrays of silicon nanowires. Physica E: Low-dimensional Systems and Nanostructures. 2007;**37**:212-217. DOI: 10.1016/j.physe.2006.09.007

[19] Palagin OV, Boyun VP, Klimovskaya AI, Belik VK. Method of Binary Addition/subtraction. Patent UA No. 107130. Bull. No. 18; 2014

[20] Palagin OV, Boyun VP, Klimovskaya AI, Belik VK. Binary Adder. Patent UA No. 107131. Bull. No. 18; 2014

[21] Lichodievskiy V, Vysotskaya N, Ryabchikov O, Korsak A, Chaikovsky Y, Klimovskaya A, et al. Application of oxidized silicon nanowires for nerve fibers regeneration. Advanced Materials Research. 2014;**854**(7):157-163. DOI: 10.4028/www.scientific.net/AMR.854.157

[22] Klimovskaya A, Vysotskaya N, Chaikovsky Y, Korsak A, Lichodievskiy V, Ostrovskii I. Morphology of the interface "silicon wire – nerve fiber". Journal of Nanoparticle Research. 2016;**39**:214-220. DOI: 10.4028/www.scientific.net/JNanoR.39.214

[23] Sarikcioglu L, Demire BM, Utuk A. Walking track analysis: An assessment method for functional recovery after sciatic nerve injury in the rat. Folia Morphologica. 2009;**68**(1):1-7. DOI: 10.4028/www.scientific.net/AMR.854.157

[24] Yu S, Kollyukh O, Ye V. Detection of dust grains vibrations with a laser heterodyne receiver of scattered light. Journal of Quantitative Spectroscopy and Radiative Transfer. 2008;**109**(8):1517-1526. DOI: 10.1016/j.jqsrt.2008.01.008

[25] Venger EF, Liptuga AI, Serozhkin Yu G. Biaxial Laser Heterodyne Displacement Meter. Patent UA No. 105679. Bull. No. 11; 2014

[26] Liptuga A, Klimovskaya A, Serozhkin Y, Likhodievskyi V, Chaikovsky Yu. Detection of nerve displacement using laser heterodyne interferometer [thesis]. Scientific and Technical Conference Laser Technologies. Lasers and Their Application (LTLA-2017); Truskavets, Ukraine; June 7-9, 2017

[27] Serozhkin Yu G, Klimovskaya AI, Chaikovsky Yu B, Lipteuga AI, Likhodiievskyi VV. Research by a Laser Heterodyne Nanodisplacements of Biological Tissues at Nerve Impulses Propagation [thesis]. The 8-st Sensor Electronics and Microsystem Technologies; Odessa, Ukraine; 28 May–1 June, 2018

[28] Sandulova V, Bogoyavlenskaya PS, Dronyuk MI. Patent USSR No. 160829. Bull. No. 5; 1964

[29] Klimovskaya AI, Ostrovskii IP, Ostrovskaya AS. Influence of growth conditions on morphology, composition, and electrical properties of n-Si wires. Physica Status Solidi A. 1996;**153**(2):465-472. DOI: 10.1002/pssa.2211530221

[30] Klimovskaya AI, Prokopenko IV, Svechnikov SV, Cherneta TG, Oberemok A, Ostrovskii IP, et al. The structure, composition, and chemical state of the surface of wire-like silicon nanocrystal grown by self-organization technology. Journal of Physics: Condensed Matter. 2002;**14**(8):1735-1743. DOI: 10.1088/0953-8984/14/8/304

[31] Serozhkin Yu G, Klimovskaya AI, Chaikovsky Yu B, Liptuga AI, Likhodiievskyi VV. Investigation of damaged nerve fibers regeneration with a laser heterodyne nanodisplacements [thesis]. The 8-st Sensor Electronics and Microsystem Technologies: Odessa, Ukraine; 28 May–1 June, 2018

[32] Aescht E, Büchl-Zimmermann S, Burmester A, Dänhardt-Pfeiffer S, Desel C, Hamers C, Jach G, Kässens M, Makovitzky J, Mulisch M, et al. Färbungen. In: Mulisch M, Welsch U, editors. Romeis Mikroskopische Technik. Heidelberg: Springer Spektrum; 2010. p. 181-297. DOI: 10.1007/978-3-8274-2254-5

[33] Naumova V, Fomin BI, Nasimov DA, Dudchenko NV, Devyatova SF, Zhanaev ED, et al. Semiconductor Science and Technology. 2010;**25**:055004. DOI: 10.1088/0268-1242/25/5/055004

[34] Ivanov Yu D, Pleshakova TO, Kozlov AF, Malsagova KA, Krohin NV, Shumyantseva VV, et al. Lab on a Chip. 2012;**12**:5104-5511. DOI: 10.1039/C2LC40555E

[35] Popov VP, Naumova OV, Ivanov Yu D. SOI nanowire transistors for femtomole electronic detectors of single particles and molecules in bioliquids and gases. In: Nazarov A, Colinge J-P, Balestra F, Raskin J-P, Gamiz F, Lysenko VS, editors. Semiconductor-On-Insulator Materials for Nanoelectronic Application. Berlin Heidelberg: Springer-Verlag; 2011. pp. 343-354. DOI: 10.1007/978-3-642-15868-1

[36] El Hady A, Machta BB. Mechanical surface waves accompany action potential propagation. Nature Communications. 2015;**6**(6697):1-7. DOI: 10.1038/ncomms7697

[37] Mueller JK, Tyler WJ. A quantitative overview of biophysical forces impinging on neural function. Physical Biology. 2014;**11**(5):051001. DOI: 10.1088/1478-3975/11/5/051001

[38] Popel' SL, Mytckan BM. Structural and morfometrics analysis of nerve fibers of sciatic nerve of rats of a different age in a norme and at hypokinesia. Journal of the Grodno State Medical University. 2016;**14**(1):60-66

[39] Tasaki I, Iwasa K. Rapid mechanical changes in crab nerve and squid axon during action potentials. Journal of Physiology. 1981;**77**(9):1055-1059, Paris

[40] Klimovskaya AI, Chaikovsky Yu B, Naumova OV, Vysotskaya NA, Korsak AV, Likhodiievsky VV, et al. Coulomb interactions at the silicon wire-nervous tissue interface. World of Medicine and Biology. 2016;**1**(55):136-141

[41] Davison SG, Levine JD, editors. Surface States. New York & London: Academic Press; 1970. pp. 94-102

[42] Gobeli CW, Allen FG. Direct and indirect excitation processes in photoelectric emission from silicon. Physics Review. 1962;**127**:141-150

[43] Allen FG, Gobeli CW. Work function, photoelectric threshold, and surface states of atomically clean silicon. Physics Review. 1962;**127**:150-159

[44] Branton D, Deamer DW. Membrane Structure. New York: Springer-Verlag Wien; 1972. pp. 6-12

[45] Logofatu C, Negrila CC, Ghita RV, Ungureanu F, Cotirlan C, Ghica C, et al. Study of SiO_2/Si interface by surface techniques. In: Basu S, editor. Crystalline Silicon–Properties and Uses. Rijeka, Croatia: InTechOpen; 2011. pp. 23-42